Journal of Electronic Research and Application, 2026, Volume 10, Issue 3
http://ojs.bbwpublisher.com/index.php/JERA
ISSN Online: 2208-3510
ISSN Print: 2208-3502

Temporal-Spatial Evolution of Proton Beam Peak Energy and Its Correlation with Plasma Density

Lu Yang

School of Physics and Astronomy, China West Normal University, Nanchong 637009, China

Abstract: In the fields of high-energy physics and particle acceleration, the peak energy of a proton beam is a core parameter for characterizing its energy properties. This paper presents a detailed discussion on the evolution of proton peak energy and its dependence on plasma density, combining theoretical research and simulations. The study integrates theoretical and simulation analyses to reveal that the peak energy of protons undergoes three distinct evolutionary stages: First, within a characteristic critical length, the variation in peak energy is independent of the channel density. Second, beyond this threshold length, the proton peak energy exhibits a rising trend over time, demonstrating a nearly linear increase with channel densities. Third, the proton peak energy does not increase indefinitely; it saturates before the protons reach the laser pulse front. Moreover, higher densities lead to earlier saturation of the peak energy. These findings provide an important foundation for future theoretical research on proton acceleration and the design of related experiments.

Keywords: Radiation pressure acceleration; Laser wakefield acceleration; High-energy proton beam; Peak energy; Plasma channel

Online publication: April 22, 2026

1. Introduction

High-energy proton beams hold broad application prospects in several key fields, such as proton imaging, fast ignition in inertial confinement fusion (ICF), medical applications and nuclear physics research [1–11]. The core of the proton transmission imaging scheme lies in the unique characteristic of the Bragg peak in the proton beam's deposition curve. It is precisely this feature that enables the practical application of proton beams in tumor therapy, offering inherent advantages such as more precise targeting of tumor cells and reduced damage to surrounding healthy tissues. Protons also play a significant role in nuclear reactions. Nuclear power plants utilize the energy released from proton interactions during nuclear fission to generate electricity, providing a viable new approach for the energy industry. Particle accelerators, as important research tools for exploring fundamental particles and forces, have achieved remarkable results in high-energy proton research. Traditional accelerators are limited by the material breakdown threshold, and their acceleration gradient is usually lower than 100 MV/m. In contrast, the acceleration gradient of laser plasma accelerators can reach times that of traditional accelerators. This

characteristic enables the accelerator to be significantly reduced in size and allows for the generation of high-energy charged particle beams over a shorter distance. Therefore, LWFA is regarded as a new type of particle acceleration method with significant development prospects.

Based on the laser plasma wakefield accelerator, researchers have proposed various acceleration mechanisms to obtain high-quality proton beams. Among them, when the laser intensity is higher than, radiation pressure acceleration (RPA) shows significant advantages. An ultra-intense laser hits a thin target, compressing electrons into a high-density electron thin layer with ponderomotive force, the electron sheath which generates a strong charge separation field that pulls and accelerates ions, a process known as RPA. Since the energy of the accelerated ions is proportional to the laser energy, using RPA to generate high-energy proton beams is one of the most promising acceleration mechanisms. Currently, research in this field mainly focuses on using circularly polarized lasers to interact with the target to achieve RPA. Compared to linearly polarized light, circularly polarized light does not have oscillating electric field components, which can effectively suppress the generation of hot electrons, thus being more conducive to achieving stable phase acceleration of ions [12–17].

The RPA still faces several key challenges in achieving high-energy proton beams. These issues mainly include limited energy acquisition during acceleration, low energy conversion efficiency from the laser field to the particle beam, and the lateral instabilities that occur during acceleration [18–20]. This instability is physically similar to the Rayleigh-Taylor instability (RTI) in fluid dynamics, which can prematurely terminate the proton acceleration process and thereby hinder the generation of high-energy proton beams. To overcome these limitations, various improved schemes for generating high-energy proton beams based on RPA have been proposed successively. Among them, the combination acceleration scheme of RPA and LWFA has attracted much attention, because in the study of the "bubble" structure of LWFA, it was found that the laser wakefield can carry extremely strong longitudinal and transverse electromagnetic fields, making it efficient for accelerating charged particles, and thus can be applied to the proton acceleration field [21–27]. Currently, the most successful scheme of the RPA and LWFA combined acceleration mechanism is to add a plasma channel behind a thin target to obtain high-energy protons. Although some studies have analyzed the effects of different laser intensity, laser pulse width and the longitudinal density distribution of the plasma channel in the laser propagation direction on the final proton energy, the quality of the high-energy proton beam, especially its peak energy evolution behavior over time, and the dependence of this behavior on the channel density parameters have not been fully explored under uniform density conditions [21–29].

This paper adopts a combined acceleration scheme of RPA and LWFA, by establishing a theoretical model and combining numerical calculations [30]. It focuses on studying the acceleration of protons in uniform plasma channels with different density parameters. The research results reveal the evolution of proton peak energy over time in the uniform plasma channels, as well as the dependence of proton peak energy on the parameters of the uniform density channels. This evolution process and the parameter dependence data are crucial for optimizing the density and length of the plasma channels in experiments, directly influencing the enhancement of proton beam energy and the control of energy dispersion. They will provide a key basis for the rational construction of the experimental model and further optimize the quality of the proton beam.

2. Theoretical model

The simulation scheme is shown in **Figure 1**. A circularly polarized Gaussian laser beam with the peak intensity of 2×10^{23}W/cm² propagates along the x-axis, it reaches the left boundary of the target at t=0 fs. The expression of

the laser is as shown in **Equation 1**, where the normalized amplitude $a_0 = eE_0/m_e\omega c = 304$, where e is the charge ω of an electron, E_0 represents the maximum amplitude of the electric field, m_e is the mass of an electron, ω represents the angular frequency of the laser, and c is the speed of light in a vacuum.

$$a(x-t) = 0.85 \times 10^{-9}\sqrt{I}\lambda_0 e^{[-(x-t)^2/t_L^2]}[\cos(x-t)\hat{y} + \sin(x-t)\hat{z}] \quad (1)$$

The laser wave-length is $\lambda_0 = 0.8\ \mu m$, the the temporal profile $t_{profile} = [\sin(\pi \times \tau_L/68)]^2$, where $0 < \tau_L < t_L$. The pulse width of the laser $t_L = 68\tau$, and $\tau = 2\pi/\omega$ represents one laser period. Within the propagation displacement range of $0 < x \leq 5\ \mu m$, there is a plasma thin target composed of protons and electrons. The density of this target is $n_1 = 10^{28}\ m^{-3}$, and it is within the critical density range $(0.1n_c < n_1 < 10n_c)$.

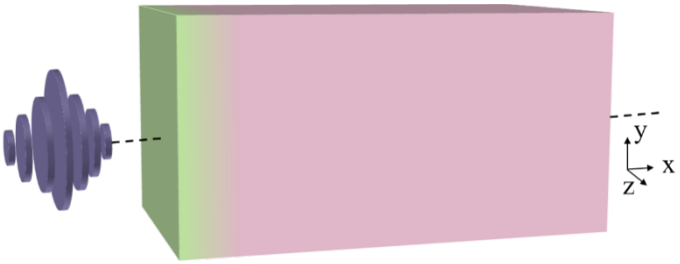

Figure 1. Combined acceleration model of RPA and LWFA driven by circular polarization laser. The green part represents a critical density thin target with a thickness of 5 μm, and the pink part represents an uniform density plasma channel.

When a circularly polarized Gaussian laser beam is applied to a critical density target, the electrons in the thin target are pushed out by the ponderomotive force of the laser to form a dense electron sheath layer. The charge separation field formed between the sheath layer and the protons in the background plasma will carry the protons out and perform pre-acceleration. This process is radiation pressure acceleration. As shown in **Figure 1**, within the range of 5 μm < x, there is a plasma channel with uniform density. When the laser pulse passes through this channel, an intense wakefield is generated. Protons are captured by the wakefield in the channel [31]. The attractive electrostatic force existing between the electron sheath layer and the protons that have undergone the previous acceleration process will pull the protons to move forward and accelerate. When the laser energy is exhausted in the plasma, the protons exit the acceleration field, indicating that the acceleration process is completed. The detailed simulation parameters are listed in **Table 1**.

Table 1. Simulation parameter configuration

Window parameters		**Plasma parameters**	
Size	$x \times y \times z$ =30×40×40 μm³	Plasma particles	Electron and proton
The number of grids	$x \times y \times z$ =600×300×300	Density	n_e =1×10²⁸ m⁻³, 0<x≤5 μm
Velocity	v =2.95×10⁸ m/s		n_e =1/2/3/5/7×10²⁶ m⁻³, 5 μm<x
Moving start time	t = 100 fs		

3. Simulation results and discussion

In this section, the three-dimensional PIC simulation was employed to investigate the dynamic process of the peak

energy evolution of protons as they are accelerated in a uniform density plasma channel by using the combined acceleration mechanism of RPA and LWFA. As shown in Figu**re 2(b)**, there is a characteristic critical length for the proton energy. Within this range (corresponding to approximately 0–330 fs in time), the change in the peak energy of the protons is independent of the density variation of the uniform plasma channel. When the time exceeds this critical point, the peak energy of protons suddenly rises sharply. Among them, when the channel density is 7×10^{26} m^{-3}, the peak energy gain is the greatest. As the density decreases, the change in proton peak energy becomes slightly more gradual. As shown in **Figure 2(c)**, when the peak energy of protons enters the density-sensitive gain stage, its peak energy shows an upward trend over time and also exhibits a nearly linear growth with the increase in channel density. The results also indicate that the higher the plasma channel density, the faster the proton peak energy increases within the same time period. It is worth noting that the increase in peak energy is not continuous and unlimited. As shown in **Figure 2(d)**, the peak energy of protons tends to saturate after reaching a certain level, indicating that the proton acceleration has ended. Specifically, when the proton is at the end of the acceleration stage in a channel with a density of 5×10^{26} m^{-3}, its peak energy shows fluctuating changes. The possible reason is that the phase between the proton beam and the laser acceleration field is not completely matched in this density channel. When the proton beam accelerates to the front of the laser field, it cannot obtain energy and will decelerate and retreat back into the acceleration field, where it is accelerated again. Therefore, the peak energy shows fluctuating changes. Furthermore, further analysis indicates that the higher the channel density, the earlier the proton peak energy reaches the saturation value. For example, when protons are captured and accelerated by the wakefield in a channel with a density of 7×10^{26} m^{-3}, the acceleration ends when time t=870. However, in a low-density channel such as 3×10^{26} m^{-3}, the protons remain in the acceleration state and still belong to the energy gain stage, indicating that the proton's dynamic behavior has not yet reached saturation. **Figure 3** show the entire process of protons from acceleration to the end in a uniform channel with a density of 3×10^{26} m^{-3}. When the laser energy is exhausted in the plasma channel or when the number of protons exceeds the laser pulse, the acceleration of protons is completed.

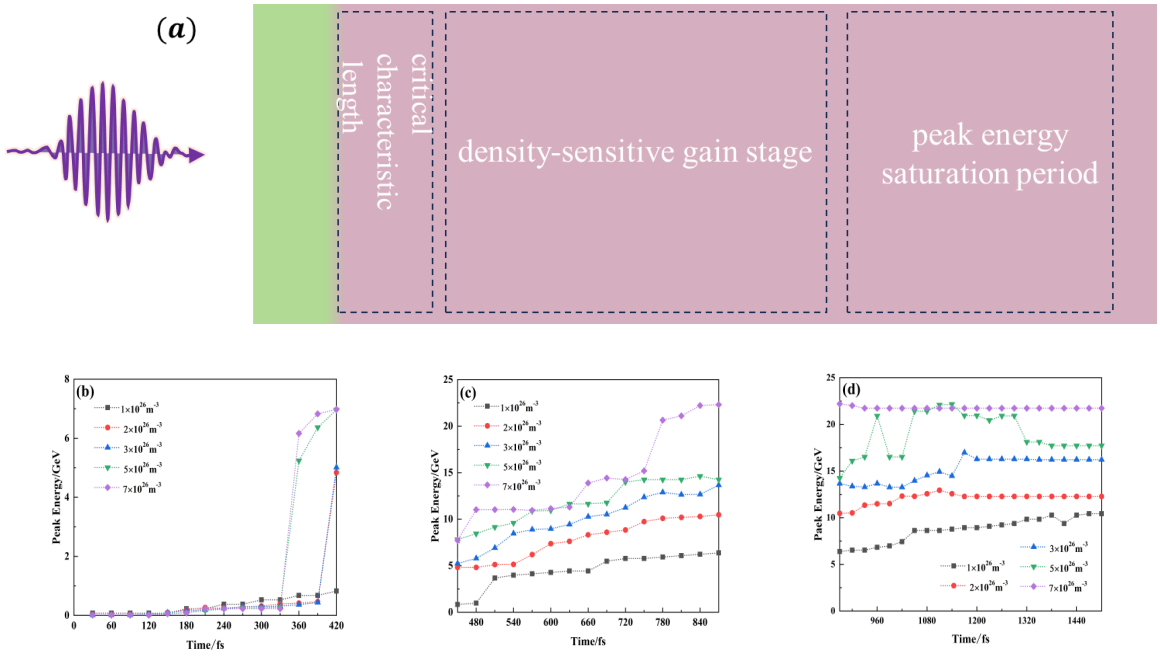

Figure 2. Evolution of proton peak energy over time in different density plasma channels. (a) Schematic diagram of the numerical simulation scheme. (b) 0–420 fs, (c) 450 fs–870 fs, (d) 900 fs–1500 fs.

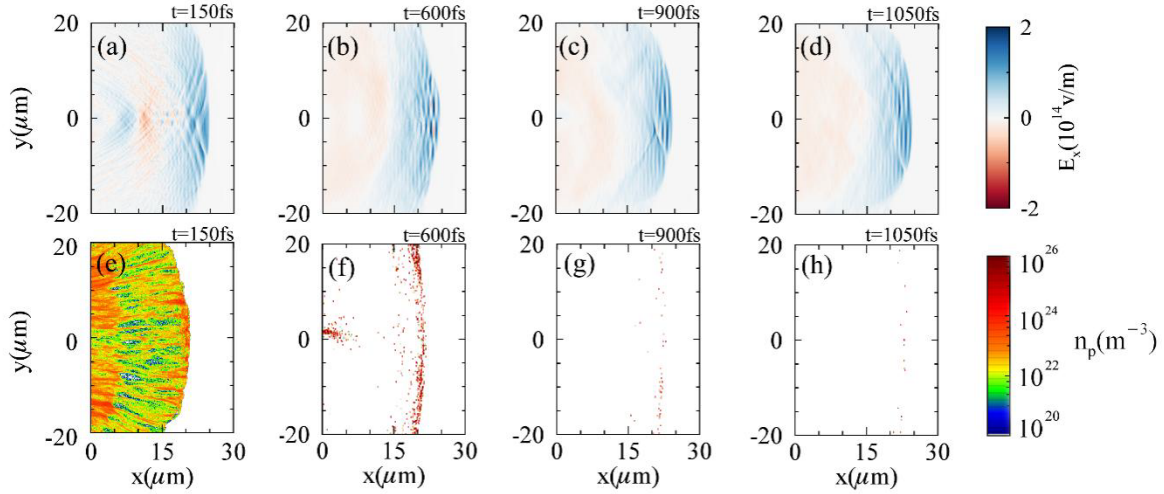

Figure 3. The acceleration of protons in a uniform density plasma channel with a density of 3×10^{20} m^{-3}. (a)–(d), (e)–(h) represent the longitudinal electric field distribution and proton density at 150 fs, 600 fs, 900 fs and 1050 fs respectively.

When accelerating protons through the combination of RPA and LWFA mechanisms, it is crucial to meet the capture conditions. In the coordinate system ($\xi = x - v_{\mathrm{wake}}t$) in which the particles are moving together with the wakefield, the motion of the ions is controlled by the conservative Hamiltonian equation [32]:

$$h\left(\xi^{'}, p_{\mathrm{i}}^{'}\right) = \gamma_w \left[\sqrt{1 + p_{\mathrm{i}}^{'2}} - p_{\mathrm{i}}^{'}\frac{v_{\mathrm{wake}}}{\mathrm{c}} - \frac{m_{\mathrm{e}} n_{\mathrm{c}} {a_0}^2}{2 m_{\mathrm{i}} n_{\mathrm{e}}}\xi^{'2}\right] \tag{2}$$

here $\xi^{'} = \xi\omega_p/\mathrm{c}$, and $p_{\mathrm{i}}^{'} = p_{\mathrm{i}}/m_{\mathrm{i}}\mathrm{c}$ are the normalized coordinates and momenta of the ions. The Lorentz factor $\gamma_w = 1/(1 - {v_{\mathrm{wake}}}^2/\mathrm{c}^2)^{1/2}$ corresponds to the phase velocity of the wakefield v_{wake}, and the v_{wake} is approximately equal to the propagation speed v_{laser} of the laser front [33,34].

$$v_{\mathrm{wake}} \simeq v_{\mathrm{laser}} \sim \exp(-4n_{\mathrm{e}}/n_{\mathrm{cr}})(1 - n_{\mathrm{e}}/n_{\mathrm{cr}})^{1/2}\mathrm{c}, \tag{3}$$

$n_{\mathrm{cr}} \simeq \left(1 + 0.48a_0^2\right)^{1/2} n_{\mathrm{c}}$, n_{cr} represents the relative near-critical density when $a_0 = 1$ for the normalized intensity of circularly polarized laser, where $n_{\mathrm{c}} = m_{\mathrm{e}}\omega^2/4\pi\mathrm{e}^2$. The equation $h\left(\xi^{'}, p_{\mathrm{i}}^{'}\right) = 1$ defines the boundary of the capture region in the phase space of $\xi^{'} - p_{\mathrm{i}}^{'}$. When the hamiltonian $\mathrm{h}\left(\xi^{'}, \mathrm{p_i}^{'}\right) < 1$, the proton can be captured by the wakefield. Through calculation, it can be known that in a plasma with a density of 1×10^{20} cm^{-3}, only relativistic ions with $p_{\mathrm{i}} \geq 1.25 m_{\mathrm{i}} c$ satisfy the capture condition $\mathrm{h}\left(\xi^{'}, p_{\mathrm{i}}^{'}\right) < 1$. In contrast, in a plasma with a density of 7×10^{20} m^{-3}, non-relativistic ions with $p_{\mathrm{i}} \approx 0.8 m_{\mathrm{i}} c$ can already enter the capture region, indicating that the higher the plasma density, the easier the proton is to be captured. From **Equation (3)**, it can be seen that as the plasma density increases, the propagation speed of the laser front decreases, and the phase velocity of the wakefield also decreases. The acceleration time of protons in the wakefield becomes shorter, and the time for the corresponding peak energy to reach the saturation value becomes earlier. This explains why protons can obtain a relatively high peak energy in a short time in the channel with a density of 7×10^{26} m^{-3}. Although the plasma wavelength $\lambda_p \propto 1/n$, when the density decreases, the bubble will become longer, delaying delaying the phase mismatch between protons and the wakefield, increasing the

acceleration distance, and ultimately the energy obtained may increase. However, it is worth noting that the efficiency of accelerating protons through the combined mechanism is jointly determined by the phase matching of the proton with the acceleration field in the laser wakefield and the distance from the laser energy depletion, and it is an integral effect in terms of distance.

4. Conclusion

In conclusion, this paper has thoroughly discussed the evolution process of proton peak energy and its dependence on density based on theoretical research and simulations. The results show that the peak energy of protons undergoes three evolution stages: Firstly, within the characteristic critical length, the change in peak energy is independent of the channel density; Secondly, beyond this threshold length, the peak energy of protons shows an upward trend over time, accompanied by an increase in channel density, presenting a nearly linear growth; Thirdly, the peak energy of protons does not increase indefinitely, before the protons reach the front of the laser pulse, it reaches saturation, and the higher the density, the earlier the peak energy reaches saturation. Eventually, a high-energy proton beam with the maximum peak energy of 22.2 GeV can be obtained. This work emphasizes that in order to achieve stable generation of high-energy proton beams using such models, a coordinated design of the plasma channel's density and length is necessary. This is a key approach to further enhance the proton beam energy and improve the beam quality, and will provide an important basis for future theoretical research on proton acceleration and related experimental design.

Disclosure statement

The authors declare no conflict of interest.

References

[1] Borghesi M, Campbell D, Schiavi A, et al., 2002, Electric Field Detection in Laser-Plasma Interaction Experiments via the Proton Imaging Technique. Physics of Plasmas, 9(5): 2214–2220.

[2] Koehler A, 1968, Proton Radiography. Science, 160(3825): 303–304.

[3] Mendel Jr C, Olsen J, 1975, Charge-Separation Electric Fields in Laser Plasmas. Physical Review Letters, 34(14): 859.

[4] Tabak M, Hammer J, Glinsky M, et al., 1994, Ignition and High Gain with Ultrapowerful Lasers. Physics of Plasmas, 1(5): 1626–1634.

[5] Naumova N, Schlegel T, Tikhonchuk V, et al., 2009, Hole Boring in a DT Pellet and Fast-Ion Ignition with Ultraintense Laser Pulses. Physical Review Letters, 102(2): 025002.

[6] Bulanov S, Khoroshkov V, 2002, Feasibility of Using Laser Ion Accelerators in Proton Therapy. Plasma Physics Reports, 2002(28): 453–456.

[7] Bulanov S, Esirkepov T, Khoroshkov V, et al., 2002, Oncological Hadrontherapy with Laser Ion Accelerators. Physics Letters A, 299(2–3): 240–247.

[8] Bulanov S, Wilkens J, Esirkepov T, et al., 2014, Laser Ion Acceleration for Hadron Therapy. Physics-Uspekhi, 57(12): 1149.

[9] Martinez B, Chen S, Bolaños S, et al., 2022, Numerical Investigation of Spallation Neutrons Generated from

Petawatt-Scale Laser-Driven Proton Beams. Matter and Radiation at Extremes, 2022, 7(2).

[10] Roth M, Jung D, Falk K, et al., 2013, Bright Laser-Driven Neutron Source based on the Relativistic Transparency of Solids. Physical Review Letters, 110(4): 044802.

[11] Ledingham K, McKenna P, Singhal R, 2003, Applications for Nuclear Phenomena Generated by Ultra-Intense Lasers. Science, 300(5622): 1107–1111.

[12] Macchi A, Cattani F, Liseykina T, et al., 2005, Laser Acceleration of Ion Bunches at the Front Surface of Overdense Plasmas. Physical Review Letters, 94(16): 165003.

[13] Robinson A, Zepf M, Kar S, et al., 2008, Radiation Pressure Acceleration of Thin Foils with Circularly Polarized Laser Pulses. New Journal of Physics, 10(1): 013021.

[14] Bulanov S, Brantov A, Bychenkov V, et al., 2008, Accelerating Monoenergetic Protons from Ultrathin Foils by Flat-Top Laser Pulses in the Directed-Coulomb-Explosion Regime. Physical Review E, 78(2): 026412.

[15] Henig A, Steinke S, Schnürer M, et al., 2009, Radiation-Pressure Acceleration of Ion Beams Driven by Circularly Polarized Laser Pulses. Physical Review Letters, 103(24): 045003.

[16] Steinke S, Hilz P, Schnürer M, et al., 2013, Stable Laser-Ion Acceleration in the Light Sail Regime. Physical Review Special Topics: Accelerators and Beams, 16(1): 011303.

[17] Kim I, Pae K, Choi I, et al., 2016, Radiation Pressure Acceleration of Protons to 93 MeV with Circularly Polarized Petawatt Laser Pulses. Physics of Plasmas, 23(7): 070701.

[18] Pegoraro F, Bulanov S, 2007, Photon Bubbles and Ion Acceleration in a Plasma Dominated by the Radiation Pressure of an Electromagnetic Pulse. Physical Review Letters, 99(6): 065002.

[19] Chen M, Pukhov A, Sheng Z, et al., 2008, Laser Mode Effects on the Ion Acceleration during Circularly Polarized Laser Pulse Interaction with Foil Targets. Physics of Plasmas, 15(11): 18–23.

[20] Liu T, Shao X, Liu C, et al., 2011, Energetics and Energy Scaling of Quasi-Monoenergetic Protons in Laser Radiation Pressure Acceleration. Physics of Plasmas, 18(12): 123105.

[21] Yu L, Xu H, Wang W, et al., 2010, Generation of Tens of GeV Quasi-Monoenergetic Proton Beams from a Moving Double Layer Formed by Ultraintense Lasers at Intensity 10 21-10 23 W cm-2. New Journal of Physics, 12(4): 045021.

[22] Liu M, Weng S, Wang H, et al., 2018, Efficient Injection of Radiation-Pressure-Accelerated Sub-Relativistic Protons into Laser Wakefield Acceleration based on 10 PW Lasers. Physics of Plasmas, 25(6): 063103.

[23] Zheng F, Wang H, Yan X, et al., 2012, Sub-TeV Proton Beam Generation by Ultra-Intense Laser Irradiation of Foil-and-Gas Target. Physics of Plasmas, 19(2): 023111.

[24] Liu M, Gao J, Wang W, et al., 2022, Theoretical Study of the Efficient Ion Acceleration Driven by Petawatt-Class Lasers via Stable Radiation Pressure Acceleration. Applied Sciences, 12(6): 2924.

[25] Zhang X, Shen B, Ji L, et al., 2010, Ultrahigh Energy Proton Generation in Sequential Radiation Pressure and Bubble Regime. Physics of Plasmas, 17(12): 123102.

[26] Tajima T, Dawson J, 1979, Laser Electron Accelerator. Physical Review Letters, 43(4): 267–270.

[27] Pukhov A, Meyer-ter-Vehn J, 2002, Laser Wake Field Acceleration: The Highly Non-Linear Broken-Wave Regime. Applied Physics B: Lasers and Optics, 74(4–5): 355–361.

[28] Bulanov S, Esarey E, Schroeder C, et al., 2015, Maximum Attainable Ion Energy in the Radiation Pressure Acceleration Regime, Laser Acceleration of Electrons, Protons, and Ions III; and Medical Applications of Laser-Generated Beams of Particles III. SPIE, 2015(9514): 34–45.

[29] Yao W, Li B, Zheng C, et al., 2016, Optimization of the Combined Proton Acceleration Regime with a Target

Composition Scheme. Physics of Plasmas, 23(1).

[30] Arber T, Bennett K, Brady C, et al., 2015, Contemporary Particle-in-Cell Approach to Laser-Plasma Modelling. Plasma Physics and Controlled Fusion, 57(11): 113001.

[31] Shen B, Xu Z, 2001, Transparency of an Overdense Plasma Layer. Physical Review. E, Statistical, Nonlinear, and Soft Matter Physics, 64(5 Pt 2): 056406.

[32] Shorokhov O, Pukhov A, 2004, Ion Acceleration in Overdense Plasma by Short Laser Pulse. Laser and Particle Beams, 22(2): 175–181.

[33] Weng S, Murakami M, Mulser P, et al., 2012, Ultra-Intense Laser Pulse Propagation in Plasmas: From Classic Hole-Boring to Incomplete Hole-Boring with Relativistic Transparency. New Journal of Physics, 14(6): 063026.

[34] Weng S, Mulser P, Sheng Z, 2012, Relativistic Critical Density Increase and Relaxation and High-Power Pulse Propagation. Physics of Plasmas, 19(2): 472.